Potential for microbial anaerobic hydrocarbon degradation in naturally petroleum-associated deep-sea sediments

Xiyang Dong [1,*], Chris Greening [2], Jayne E. Rattray [1], Anirban Chakraborty [1], Maria Chuvochina[2,3], Daisuke Mayumi [1,4], Carmen Li [1], James M. Brooks [5], Bernie B. Bernard [5], Ryan A. Groves[1], Ian A. Lewis [1], Casey R.J. Hubert [1,*]

[1] Department of Biological Sciences, University of Calgary, Calgary, T2N 1N4, Canada

[2] School of Biological Sciences, Monash University, Clayton, VIC 3800, Australia

[3] Australian Centre for Ecogenomics, School of Chemistry and Molecular Biosciences, The University of Queensland, QLD 4072, Australia

[4] Institute for Geo-Resources and Environment, Geological Survey of Japan, National Institute of Advanced Industrial Science and Technology (AIST), 1-1-1 Higashi, Tsukuba, 305-8567, Japan

[5] TDI Brooks International, College Station, Texas, TX 77845, USA

* Corresponding authors. E-mail: xiyang.dong@ucalgary.ca (X. Dong), chubert@ucalgary.ca (C. R.J. Hubert).

The authors declare no conflict of interest.

Abstract

The lack of cultured isolates and microbial genomes from the deep seabed means that very little is known about the ecology of this vast habitat. Here, we investigated energy and carbon acquisition strategies of microbial communities from three deep seabed petroleum seeps (3 km water depth) in the Eastern Gulf of Mexico. Shotgun metagenomic analysis revealed that each sediment harbored diverse communities of chemoheterotrophs and chemolithotrophs. We recovered 82 metagenome-assembled genomes affiliated with 21 different archaeal and bacterial phyla. Multiple genomes encoded enzymes for acetogenic fermentation of aliphatic and aromatic compounds, specifically those of candidate phyla *Aerophobetes*, *Aminicenantes*, TA06 and *Bathyarchaeota*. Microbial interactions in these communities are predicted to be driven by acetate and molecular hydrogen, as indicated by a high abundance of fermentation, acetogenesis, and hydrogen utilization pathways. These findings are supported by sediment geochemistry, metabolomics and thermodynamic modelling of hydrocarbon degradation. Overall, we infer that deep-sea sediments experiencing thermogenic hydrocarbon inputs harbor phylogenetically and functionally diverse communities potentially sustained through anaerobic hydrocarbon, acetate and hydrogen metabolism.

Deep-sea sediments, generally understood to be those occurring in water depths greater than ~500 meters, represent one of the largest habitats on Earth. In recent years, culture-independent 16S rRNA gene surveys and metagenomic studies have revealed these sediments host a vast abundance and diversity of bacteria and archaea [1-8]. Cell numbers decrease with sediment depth and age, from between 10^6 and 10^{10} cm^{-3} in the upper cm at the sediment-water interface to below 10^4 cm^{-3} several kilometers below the ocean floor [9, 10]. However, due to a lack of cultured representatives and genomes recovered from deep-sea sediments, it remains largely unresolved how microorganisms survive and function in these nutrient-limited ecosystems. Energy and carbon sources are essential requirements that allow the buried microorganisms to persist. With sunlight penetration not reaching the deep seabed, photosynthetic processes do not directly support these communities [11]. It has therefore been proposed that deep sea benthic and subsurface microbes are primarily sustained by complex detrital organic matter, including carbohydrates, proteinaceous compounds, and humic substances, derived from the overlying water column via sedimentation [11-13].

Another important potential carbon and energy source in deep-sea sediments are petroleum geofluids that migrate from subseafloor reservoirs up to the seafloor [14]. Petroleum compounds include smaller gaseous molecules, such as methane, propane and butane, and larger aliphatic and aromatic liquids. Numerous studies have investigated the role of methane oxidation in seabed sediments, which is mediated by anaerobic methanotrophic archaea (ANME), generally in syntrophy with bacteria respiring sulfate or other electron acceptors [4, 6, 8, 15, 16]. In contrast, little is known about the degradation of larger alkanes or aromatic compounds by deep seabed microorganisms. Vigneron et al. [2] performed a comparative gene-centric study of hydrocarbon and methane seeps of the Gulf of Mexico, and suggested that microorganisms in deep cold seeps

(water depth ~1 km) can potentially utilize a range of non-methane hydrocarbons. However, due to the absence of metagenome binning in that study, relevant metabolic functions were not assigned to specific pathways or taxa.

In addition to organic carbon compounds, microbial life in deep-sea sediments is also supported by inorganic electron donors. Some microorganisms have been isolated from deep sediments that are able to sustain themselves by oxidizing elemental sulfur, hydrogen sulfide, carbon monoxide, ammonia and molecular hydrogen (H_2) [6, 8, 11]. Of these, H_2 is a particularly important energy source given its production in large quantities by biological and geochemical processes. H_2 can be generated as a metabolic byproduct of fermentation, together with volatile fatty acids such as acetate, during organic matter degradation [9, 17]. H_2 can also be produced abiotically via serpentinization, radiolysis of water, or thermal alteration of sedimentary organic matter [18]. For example, the radiolysis of water by naturally occurring radionuclides (*e.g.* ^{40}K and ^{238}U) is estimated to produce 10^{11} mol H_2 per year [8, 19]. Depending on the availability of electron acceptors, H_2 oxidation can be coupled to sulfate, nitrate, metal, and organohalide respiration, as well as acetogenesis and methanogenesis [8, 11].

To develop understanding of the role of hydrocarbon substrates metabolic processes in supporting microbial life in deep-sea sediments, we performed metagenomic, geochemical and metabolomic analyses of three deep seabed sediments (water depth ~3km). The three sites exhibited different levels of migrated thermogenic hydrocarbons. Metagenomes generated from sediment samples of each site were assembled and binned to obtain metagenome-assembled genomes (MAGs) and to reconstruct metabolic pathways for dominant members of the microbial communities. Complementing this genome-resolved metagenomics, a gene-centric analysis was

79 performed by directly examining unassembled metagenomic data. Through the combination of
80 metagenomics with geochemistry and metabolomics, with supporting thermodynamic modeling,
81 we provide evidence that (1) deep-sea sediments harbor phylogenetically diverse heterotrophic
82 and lithotrophic microbial communities; (2) some members from the candidate phyla are
83 engaged in degradation of aliphatic and aromatic thermogenic hydrocarbons; and (3) microbial
84 community members are likely interconnected via acetate and hydrogen metabolism.

85 **Results**

86 **Sediment geochemistry**

87 This study tested three petroleum-associated near-surface sediments (referred to as Sites E26,
88 E29 and E44) sampled from the Eastern Gulf of Mexico [20]. Petroleum content and other
89 geochemical characteristics were analyzed for each of the three sites (Table 1). All sites had high
90 concentrations of aromatic compounds and liquid alkanes; aromatic compounds were most
91 abundant at Site E26, while liquid alkanes were at 2.5-fold higher concentration at Sites E26 and
92 E29 than Site E44. Alkane gases were only abundant at Site E29 and were almost exclusively
93 methane (CH_4). CH_4 sources can be inferred from stable isotopic compositions of CH_4 and molar
94 ratios of CH_4 to higher hydrocarbons [15]. Ratios of $C_1/(C_2+C_3)$ were greater than 1,000 and $\delta^{13}C$
95 values of methane were more negative than -60‰, indicating that the CH_4 in these sediments is
96 predominantly biogenic [15, 21]. GC-MS revealed an unresolved complex mixture (UCM) of
97 saturated hydrocarbons in the C_{15+} range in all three sites. Such UCM signals correspond to
98 degraded petroleum hydrocarbons and may indicate the occurrence of oil biodegradation at these
99 sites [22]. Signature metabolites for anaerobic biodegradation of alkanes and aromatic compounds
100 [23] were also detected, including benzoate, toluate and methyl- or trimethylsilyl esters (Table S1).

High concentrations of sulfate (>20 mM) were detected at each of the three sites (Table 1), consistent with sulfate being present in high concentrations in seawater and diffusing into the sediments. H_2 and acetate concentrations were both below limits of detection (0.015-0.1 nM and 2.5 µM, respectively); this is consistent with previous observations in deep-sea sediments showing that H_2 and acetate is present at extremely low steady-state concentrations due to tight coupling between producers and consumers [3, 15].

Deep-sea sediments harbor phylogenetically diverse bacterial and archaeal communities

Illumina NextSeq sequencing of genomic DNA from deep-sea sediment communities produced 85,825,930, 148,908,270, and 138,795,692 quality-filtered reads for Sites E26, E29, and E44, respectively (Table S2). The 16S rRNA gene amplicon sequencing results suggest the sediments harbor diverse bacterial and archaeal communities, with Chao1 richness estimates of 359, 1375 and 360 amplicon sequence variants (ASVs) using bacterial-specific primers, and 195, 180 and 247 ASVs using archaeal-specific primers, for Sites E26, E29 and E44, respectively (Table S3 and Figure S1). Taxonomic profiling of these metagenomes using small subunit ribosomal RNA (SSU rRNA) marker genes demonstrated that the most abundant phyla in the metagenomes were, in decreasing order, *Chloroflexi* (mostly classes *Dehalococcoidia* and *Anaerolineae*), *Candidatus* Atribacteria, *Proteobacteria* (mostly class *Deltaproteobacteria*), and *Candidatus* Bathyarchaeota (Figure 1a). While the three sites share a broadly similar community composition, notable differences were *Ca.* Bathyarchaeota and *Proteobacteria* being in higher relative abundance at the sites with more hydrocarbons (E29 and E26; Table 1), whereas the inverse is true for *Actinobacteria*, the Patescibacteria group, and *Ca.* Aerophobetes that are all present in higher relative abundance at Site E44 where hydrocarbon levels are lower. Additional sampling is

123 required to determine whether these differences are due to the presence of hydrocarbons or other
124 factors.

125 Assembly and binning for the three metagenomes resulted in a total of 82 MAGs with >50%
126 completeness and <10% contamination based on CheckM analysis [24]. Reconstructed MAGs
127 comprise taxonomically diverse members from a total of six archaeal and 15 bacterial phyla
128 (Figure 2 and Table S4). Within the domain Bacteria, members of the phylum *Chloroflexi* are
129 highly represented in each sample, especially from the classes *Dehalococcoidia* and
130 *Anaerolineae*. Within the domain Archaea, members of phylum *Bathyarchaeota* were recovered
131 from all three sites. Most other MAGs belong to poorly understood candidate phyla that lack
132 cultured representatives, including *Aminicenantes* (formerly OP8), *Aerophobetes* (formerly
133 CD12), *Cloacimonas* (formerly WWE1), *Stahlbacteria* (formerly WOR-3), *Atribacteria*
134 (formerly JS1 and OP9), TA06 and the Asgard superphylum including *Lokiarchaeota*,
135 *Thorarchaeota*, and *Heimdallarchaeota*.

136 Among those phyla, candidate phylum TA06 is the only one not yet given provisional names.
137 Also known as GN04 or AC1, it was originally discovered in a hypersaline microbial mat [25].
138 First genomic representatives of this phylum were recovered from estuarine sediments [26] with a
139 small number of other MAGs recently reported to belong to this lineage [27, 28]. Due to the paucity
140 of available MAGs and misclassifications based on 16S rRNA gene sequences, members of
141 TA06 are often 'confused' with members of the phylum WOR-3 (*Stahlbacteria*) [28]. In addition to
142 the phylogenetic inference here based on 43 concatenated protein marker genes (Figure 2), the
143 placement of two bins within the original TA06 phylum is further supported by genome

144 classification based on concatenation of 120 ubiquitous, single-copy marker genes [29] as well as
145 classification of 16S rRNA genes using the SILVA database [30] (Tables S4 and S5).

146 In summary, while there are considerable community-level differences between the three sample
147 locations, the recovered MAGs share common taxonomic affiliations at the phylum and class
148 levels. Guided by sediment geochemistry (Table 1), we subsequently analyzed the metabolic
149 potential of these MAGs to understand how bacterial and archaeal community members generate
150 energy and biomass in these natural petroleum-associated deep-sea environments. Hidden
151 Markov models (HMMs) and homology-based models were used to search for the presence of
152 different metabolic genes in both the recovered MAGs and unbinned metagenomes. Where
153 appropriate, findings were further validated through metabolomic analyses, phylogenetic
154 visualization, and analysis of gene context.

155 **Capacity for detrital biomass and hydrocarbon degradation in sediment microbial**
156 **communities**

157 In deep-sea marine sediments organic carbon is supplied either as detrital matter from the
158 overlying water column or as aliphatic and aromatic petroleum compounds that migrate upwards
159 from underlying petroleum-bearing sediments [11]. With respect to detrital matter, genes involved
160 in carbon acquisition and breakdown were prevalent across both archaeal and bacterial MAGs.
161 These include genes encoding intracellular and extracellular carbohydrate-active enzymes and
162 peptidases, as well as relevant transporters and glycolysis enzymes (Figure 3 and Table S6). The
163 importance of these carbon acquisition mechanisms is supported by the detection of
164 corresponding intermediate metabolites, such as glucose and amino acids, in all three sediments
165 (Table S1). The ability to break down fatty acids and other organic acids via the beta-oxidation

166 pathway was identified in 13 MAGs, including members of *Chloroflexi*, *Deltaproteobacteria*,
167 *Aerophobetes* and *Lokiarchaeota* (Figure 3 and Table S6). These results align with many other
168 studies suggesting that the majority of seabed microorganisms are involved in recycling of
169 residual organic matter, including complex carbohydrates, proteins and lipids [13, 31, 32].

170 Unlike in other studies, the presence of petroleum hydrocarbons is a defining feature of the
171 sediments investigated here and thus a key goal of this study was to identify the potential for
172 microbial degradation of hydrocarbons as a source of energy and carbon. To this end, we focused
173 on functional marker genes encoding enzymes that catalyze the activation of mechanistically
174 sophisticated C-H bonds, to initiate hydrocarbon biodegradation [33]. For anaerobic hydrocarbon
175 degradation, four oxygen-independent C-H activation reactions have been characterized: (1)
176 addition of fumarate by glycyl-radical enzymes, *e.g.* for activation of alkylbenzenes and
177 straight chain alkanes [34]; (2) hydroxylation with water by molybdenum cofactor-containing
178 enzymes, *e.g.* for activation of ethylbenzene [33]; (3) carboxylation catalyzed by UbiD-like
179 carboxylases, *e.g.* for activation of benzene and naphthalene [35]; and (4) reverse methanogenesis
180 involving variants of methyl-coenzyme M reductase, *e.g.* for activation of methane and butane
181 [36]. Most of the evidence for mechanisms (1) – (3) has come from studies of hydrocarbon
182 contaminated aquifers, whereas mechanism (4) has been studied extensively in marine sediments
183 [23, 37].

184 Evidence for glycyl-radical enzymes that catalyze fumarate addition was found in 15 out of the
185 82 MAGs based on identifying genes encoding alkylsuccinate synthase (AssA) (Figures 3 and
186 4a). The *assA* sequences identified, while phylogenetically distant from canonical fumarate-
187 adding enzymes and pyruvate formate lyases (Pfl), form a common clade with Pfl-like AssA

from *Archaeoglobus fulgidus* VC-16 and *Abyssivirga alkaniphila* L81 (Figure 4a). Both of these organisms have been shown experimentally to be capable of anaerobic alkane degradation [38, 39]. The putative *assA* genes identified here are present in all three samples regardless of hydrocarbon concentrations. They belong to MAGs affiliated with the bacterial phyla *Aerophobetes*, *Aminicenantes* and *Chloroflexi* as well as the archaeal phyla *Bathyarchaeota*, *Lokiarchaeota* and *Thorarchaeota*. The highest relative abundance of putative *assA* sequences was found in Site E29 as indicated by quality-filtered reads, which is consistent with this sediment containing the highest concentration of aliphatic compounds (Tables 1 and S7). Additional searching for other genes encoding fumarate-adding enzymes in the quality-filtered reads (e.g. *bssA*, *nmsA*, and canonical *assA*) did not return significant counts (Figure 4 and Table S7). Among the other three anaerobic hydrocarbon biodegradation mechanisms mentioned above, a MAG classified as *Dehalococcoidia* (*Chloroflexi* E29_bin2) contained genes encoding putative catalytic subunits of *p*-cymene dehydrogenase (Cmd) and alkane C_2-methylene hydroxylase (Ahy) (Figures 3 and S2), known to support *p*-cymene and alkane utilization [37]. Genes encoding enzymes catalyzing hydrocarbon carboxylation, reverse methanogenesis and aerobic hydrocarbon degradation (e.g. *alkB*, *nahC* and *nahG*) were not detected (Table S6). The latter result is expected due to the low concentrations of oxygen in the top 20 cm of organic rich seabed sediments [11].

Considering the degradation of aromatic hydrocarbons, genes responsible for reduction of benzoyl-CoA were detected in 12 MAGs (Figures 3 and 4b). Benzoyl-CoA is a universal biomarker for anaerobic degradation of monoaromatic compounds as it is a common intermediate to biochemical pathways catalyzing this process [40]. Benzoyl-CoA reduction to cyclohex-1,5-diene-1-carboxyl-CoA is performed by Class I ATP-dependent benzoyl-CoA

reductase (BCR; BcrABCD) in facultative anaerobes (*e.g. Thauera aromatica*) or Class II ATP-independent reductase (Bam; BamBCDEFGHI) in strict anaerobes like sulfate reducers [41]. The *bcr* genes detected are all Class I, and were found in bacterial MAGs (*i.e.*, *Dehalococcoidia*, *Anaerolineae*, *Deltaproteobacteria*, *Aminicenantes* and TA06) and archaeal MAGs (*i.e.*, *Thermoplasmata* and *Bathyarchaeota*) (Figures 3 and 4b). Genes for further transformation of dienoyl-CoA to 3-hydroxypimelyl-CoA were also identified (Figures 3 and 4b), *i.e.*, those encoding 6-oxo-cyclohex-1-ene-carbonyl-CoA hydrolase (Oah), cyclohex-1,5-diencarbonyl-CoA hydratase (Dch) and 6-hydroxycyclohex-1-ene-1-carbonyl-CoA dehydrogenases (Had) [42]. Together with the detection of 23 – 162 nM benzoate in these sediments (Table 1) these results strongly suggest that the organisms represented by these MAGs mediate the typical downstream degradation of aromatic compounds through the central benzoyl-CoA Bcr-Dch-Had-Oah pathway. However, the upstream pathways resulting in benzoate production from degradation of complex aromatic compounds were not resolved based on current data.

Widespread capacity for fermentative production and respiratory consumption of acetate and hydrogen

Analysis of MAGs from these deep-sea hydrocarbon-associated sediments suggests that fermentation, rather than respiration, is the primary mode of organic carbon turnover in these environments. Most recovered MAGs with capacity for heterotrophic carbon degradation lacked respiratory primary dehydrogenases and terminal reductases, with exceptions being several *Proteobacteria* and one *Chloroflexi* (Table S6). In contrast, 6 and 14 MAGs contained genes indicating the capability for fermentative production of ethanol and lactate, whereas some 69 MAGs contained genes for fermentative acetate production (Figure 3 and Table S6). These

findings are consistent with other studies emphasizing the importance of fermentation, including acetate production, in deep-sea sediments [12, 43].

Acetate can also be produced by acetogenic CO_2 reduction through the Wood-Ljungdahl pathway using a range of substrates, including heterotrophic compounds [15]. Partial or complete sets of genes for the Wood-Ljungdahl pathway were found in 50 MAGs (Figures 3 and S3), including those affiliated with phyla previously inferred to mediate acetogenesis in deep-sea sediments through either the tetrahydrofolate-dependent bacterial pathway (*e.g. Chloroflexi* and *Aerophobetes*) [7, 44] or the tetrahydromethanopterin-dependent archaeal variant (*e.g. Bathyarchaeota* and Asgard group) [45, 46]. In addition, the signature diagnostic gene for the Wood-Ljungdahl pathway (*acsB*; acetyl-CoA synthase) is in high relative abundance in the quality-filtered metagenome reads at all three sites (Table S7). These observations are in agreement with mounting evidence that homoacetogens play a quantitatively important role in organic carbon cycling in the marine deep biosphere [45, 47, 48].

Evidence for H_2 metabolism was also found in MAGs from all three sites. We screened putative hydrogenase genes from various subgroups in MAGs as well as unbinned metagenomic sequences (Figures 1, 3 and Tables S6, S7). Surprisingly few H_2 evolving-only hydrogenases were detected, with only five Group A [FeFe]-hydrogenases and five Group 4 [NiFe]-hydrogenases detected across the bacterial and archaeal MAGs. Instead, the most abundant hydrogenases within the MAGs and quality-filtered unassembled reads were the Group 3b, 3c, and 3d [NiFe]-hydrogenases. Group 3b and 3d hydrogenases are physiologically reversible, but generally support fermentation in anoxic environments by coupling NAD(P)H reoxidation to fermentative H_2 evolution [49-51]. Group 3c hydrogenases mediate a central step in

hydrogenotrophic methanogenesis, bifurcating electrons from H_2 to heterodisulfides and ferredoxin [52]; their functional role in Bacteria and non-methanogenic Archaea remains unresolved [51] yet their corresponding genes co-occur with heterodisulfide reductases across multiple archaeal and bacterial MAGs (Figure 3). Various Group 1 [NiFe]-hydrogenases were also detected, which are known to support hydrogenotrophic respiration in conjunction with a wide range of terminal reductases. This is consistent with previous studies in the Gulf of Mexico that experimentally measured the potential for hydrogen oxidation catalyzed by hydrogenase enzymes [53].

Given the genomic evidence for hydrogen and acetate production in these sediments, we investigated whether any of the MAGs encoded terminal reductases to respire using these compounds as electron donors. In agreement with the high sulfate concentrations (Table 1), the key genes for dissimilatory sulfate reduction (*dsrAB*) were widespread across the metagenome reads, particularly at Site E29 (Table S7). These genes were recovered from MAGs affiliated with *Deltaproteobacteria* and *Dehalococcoidia* (Table S6). We also identified 31 novel reductive dehalogenase (*rdhA*) genes across 22 MAGs, mainly from *Aminicenantes* and *Bathyarchaeota* (Figure 3 and Table S6), suggesting that organohalides – that can be produced through abiotic and biotic processes in marine ecosystems [54] – may be electron acceptors in these deep-sea sediments. All MAGs corresponding to putative sulfate reducers and dehalorespirers encoded the capacity to completely oxidize acetate and other organic acids to CO_2 using either the reverse Wood-Ljungdahl pathway or TCA cycle (Figure 3 and Table S6). Several of these MAGs also harbored the capacity for hydrogenotrophic dehalorespiration *via* Group 1a and 1b [NiFe]-hydrogenases (Figure 3). In addition to these dominant uptake pathways, one MAG belonging to the epsilonproteobacterial genus *Sulfurovum* (E29_bin29) included genes for the enzymes

needed to oxidize either H_2 (group 1b [NiFe]-hydrogenase), elemental sulfur (SoxABXYZ), and sulfide (Sqr), using nitrate as an electron acceptor (NapAGH); this MAG also has a complete set of genes for autotrophic CO_2 fixation *via* the reductive TCA cycle (Figure 3 and Table S6).). In contrast, the capacity for methanogenesis appears to be relatively low and none of the MAGs contained *mcrA* genes. The genes for methanogenesis were detected in quality-filtered unassembled reads in all three sediments (Figures 1d and S4) and were mainly affiliated with acetoclastic methanogens at Site E29, and hydrogenotrophic methanogens at the other two sites (Figures 1d and S4). Overall, the collectively weak *mcrA* signal in the metagenomes suggests that the high levels of biogenic methane detected by geochemical analysis (Table 1) is primarily due to methanogenesis in sediment layers deeper than the top 20 cm.

Thermodynamic modelling of hydrocarbon degradation

Both the geochemistry data and biomarker gene survey suggest that hydrocarbon degradation occurs in the three deep-sea sediments sampled (Tables 1 and S1). Recreating the environmental conditions for cultivating the organisms represented by the retrieved MAGs is a challenging process, preventing further validation of the hydrocarbon degradation capabilities (and other metabolisms) among the majority of the lineages represented by the MAGs retrieved here [48]. Instead, we provide theoretical evidence that hydrocarbon degradation is feasible in this environment by modelling whether these processes are thermodynamically favorable in the conditions typical of deep sea sediments, namely high pressure and low temperature.

As concluded from the genome analysis and supported by metabolomics (Table 1), it is likely that most hydrocarbon oxidation occurs through fermentation rather than respiration. Taking hydrogen production and the Wood-Ljungdahl pathway into consideration (Figures 3 and 4), we

compared the thermodynamic constraints on hydrocarbon biodegradation for two plausible scenarios: (1) fermentation with production of hydrogen and acetate, and (2) fermentation with production of acetate alone. Hexadecane and benzoate are used as representative aliphatic and aromatic compounds, respectively, based on the geochemistry results (e.g. C_{2+} alkane detection) and genomic analysis (e.g. *bcr* genes) [47, 55]. The calculated results show that the threshold concentrations of acetate that result in favorable energetics ($\Delta G' < 0$ kJ mol^{-1}) for fermentative co-generation of acetate and hydrogen require acetate to be extremely low in a hexadecane degradation scenario ($< 10^{-12}$ mM acetate) and acetate to be at moderate levels in a benzoate degradation scenario (< 3.8 mM acetate) (Figure 5). By contrast, for fermentation leading to production of only acetate, its concentration can be as high as 470 mM in a benzoate degradation scenario and as high as 300 mM in a hexadecane degradation scenario (Figure 5). Fermentative degradation of hexadecane to hydrogen and acetate in the deep seabed could therefore be less favorable than acetate production alone via the Wood-Ljungdahl pathway Thus, if microbial communities consume hexadecane or more complex hydrocarbons as carbon and energy sources, it is likely that they employ the Wood-Ljungdahl pathway to produce acetate. However, other reactions such as fermentation to H_2 still cannot be excluded, *e.g.*, for less complex hydrocarbons such as benzoate and related compounds.

Discussion

In this study, metagenomics revealed that most of the Bacteria and Archaea in the deep-sea sediment microbial communities sampled belong to candidate phyla that lack cultured representatives and sequenced genomes (Figures 1 and 2). As a consequence, it is challenging to link phylogenetic patterns with the microbial functional traits underpinning the biogeochemistry

of deep seabed habitats. Here, we were able to address this by combining *de novo* assembly and binning of metagenomic data with geochemical and metabolomic analyses, and complementing our observations with thermodynamic modeling. Pathway reconstruction from 82 MAGs recovered from the three deep-sea near surface sediments revealed that many community members were capable of anaerobic hydrocarbon degradation as well as acquiring and hydrolyzing residual organic matter (Figure 3), whether supplied as detritus from the overlying water column or as autochthonously produced necromass (Figure 6). Heterotrophic fermenters and acetogens were in considerably higher relative abundance than heterotrophic respirers, despite the abundance of sulfate in the sediments (Table 1). For example, while genomic coverage of putative sulfate reducers is relatively low (< 1% of the communities), the most abundant MAG at each site were all putative acetogenic heterotrophs, *i.e. Dehalococcoidia* E26_bin16, *Actinobacteria* E44_bin5, and *Aminicenantes* E29_bin47 for Sites E26, E44 and E29 respectively (~3.3-4.5% relative abundance, Table S4). Therefore, in contrast with coastal sediments [56], microbial communities in the deep seabed are likely influenced by the capacity to utilize available electron donors more so than by the availability of oxidants.

In this context, multiple lines of evidence indicate degradation of aliphatic or aromatic petroleum compounds as carbon and energy sources for anaerobic populations in these deep-sea hydrocarbon seep environments (Table 1, Figures 3 - 5). Whereas capacity for detrital organic matter degradation is a common feature in the genomes retrieved in this study, and from many other environments [26], anaerobic hydrocarbon degradation is a more exclusive feature that was detected in 23 out of 82 MAGs. Evidence of anaerobic alkane oxidation via fumarate addition and hydroxylation pathways, as well as anaerobic aromatic compound degradation by the Class I benzoyl-CoA reductase pathway, was found in all three sediments. The ability to utilize

hydrocarbons may explain the ecological dominance (high relative abundance) of certain lineages of Bacteria and Archaea in these microbial communities (Figure 1a), as many of those phyla have previously been found to be associated with hydrocarbons in various settings. For example, *Aerophobetes* have been detected in other cold seep environments [7], *Aminicenantes* are often found associated with fossil fuels [27], and *Chloroflexi* harboring genes for anaerobic hydrocarbon degradation have been found in hydrothermal vent sediments [4]. While Archaea have been reported to mediate oxidation of methane and other short-chain alkanes in sediments [5, 36], few have been reported to anaerobically degrade larger hydrocarbons [37]. The finding of *Bathyarchaeota* and other archaeal phyla potentially capable of anaerobic hydrocarbon degradation extends the potential hydrocarbon substrate spectrum for Archaea. More broadly, these findings extend the breadth of bacterial and archaeal lineages that putatively degrade hydrocarbons. Current knowledge of anaerobic hydrocarbon degradation remains limited, with the majority of studies focused on environments subject to anthropogenic hydrocarbon contamination, most notably groundwater aquifers [37]. It is possible that microorganisms inhabiting deep-sea sediments harbor novel mechanisms for anaerobic hydrocarbon degradation that may be relevant for biotechnology and bioremediation in a variety of other settings, *e.g.*, other cold habitats. Future studies of genome-enabled hydrocarbon degradation using samples such as the sediments studied here may elucidate this further.

Genomic analyses of 12 MAGs harboring genes for central benzoyl-CoA pathway reveal that they are likely a mixture of obligate fermenters and sulfate reducers. The finding that these organisms use the ATP-consuming class I, not the reversible class II, benzoyl-CoA reductase is surprising. It is generally thought that strict anaerobes must use class II BCRs because the amount of energy available from benzoate oxidation during sulfate reduction or fermentation is

368 not sufficient to support the substantial energetic requirement of the ATP-dependent class I BCR
369 reaction [42]. However, acetogenic fermentation of hydrocarbons may explain how the Class I
370 reaction could be thermodynamically favorable, as shown in Figure 5. In agreement with this,
371 there are reported exceptions to the general Class I vs Class II observations, such as the
372 hyperthermophilic archaeon *Ferroglobus placidus* that couples benzoate degradation via the
373 Class I system with iron reduction [42], and fermentative deep-sea *Chloroflexi* strains DscP3 and
374 Dsc4 that contain genes for class I benzoyl-CoA reductases [44]. Indeed, acetogens can utilize
375 many different substrates and have relatively high ATP yields, as well as thermodynamic
376 efficiencies toward heterotrophic substrates, which is consistent with the proposed importance of
377 acetogens in energy-limited seafloor ecosystems [45, 47].

378 Based on the evidence presented here, we propose that acetate and hydrogen are the central
379 intermediates underpinning community interactions and biogeochemical cycling in these deep-
380 sea sediments (Figure 6). Maintaining low acetate and hydrogen concentrations in the
381 environment is important for promoting continuous fermentation of organic substrates, consistent
382 with thermodynamic constraints (Figure 5). Acetate and hydrogen in sediment porewater were
383 below detection limits, consistent with the high turnover rates of both compounds. This may
384 correspond with the genomic potential within these microbial communities for the coupling of
385 acetate consumption to sulfate reduction, organohalide respiration and acetoclastic
386 methanogenesis, as suggested in other studies [55, 57]. Some community members also appear to be
387 capable of H_2 consumption, including *via* putative heterodisulfide reductase-coupled
388 hydrogenases. In turn, hydrogen oxidation can support autotrophic carbon fixation and therefore
389 may provide a feedback loop for regeneration of organic carbon. Acetate- and hydrogen-

oxidizing community members are likely to promote upstream fermentative degradation of necromass and hydrocarbons (Figure 6).

Overall, this metagenome dataset extended the knowledge of metabolic potential of microbial communities inhabited in deep-sea sediments that receive an input of thermogenic hydrocarbon. They are mostly likely sustained through fermentation, acetogenesis and hydrogen metabolisms. More importantly, as supported by geochemical data, metabolomic analysis, and thermodynamic modelling, our findings expand the diversity of microbial lineages with the potential for anaerobic hydrocarbon degradation through *e.g.* the activity of glycyl-radical enzymes. Together with the recent discovery of anaerobic butane degradation in gas-rich hydrothermally-heated sediments [36], it can be inferred that anaerobic degradation of hydrocarbons heavier than methane might be more widespread than previously expected and may significantly contribute to energy and carbon budgets in dark deep-sea sediments [58].

Methods

Sampling and geochemical measurements

The three marine sediment samples used in this study were collected from the near-surface (top 20 cm) of the seafloor in the Eastern Gulf of Mexico as part of a piston coring survey, as described previously [20]. Samples for hydrocarbon characterization were sectioned on board the research vessel immediately following piston core retrieval, flushed with N_2 and sealed in hydrocarbon-free gas tight metal canisters then frozen until analysis. Interstitial gas analysis was later performed on the headspace in the canisters using GC with Flame Ionization Detector (GC-FID). Sediment samples for gas/liquid chromatography and stable isotope analysis were frozen,

411 freeze-dried and homogenized then extracted using accelerated solvent extraction (ACE 200).
412 Extracts were subsequently analyzed using GC/FID, a Perkin-Elmer Model LS 50B fluorometer,
413 GC/MS and Finnigan MAT 252 isotope mass spectrometry as detailed elsewhere [59].

414 Sulfate and chloride concentrations were measured in a Dionex ICS-5000 reagent-free ion
415 chromatography system (Thermo Scientific, CA, USA) equipped with an anion-exchange
416 column (Dionex IonPac AS22; 4 × 250 mm; Thermo Scientific), an EGC-500 K_2CO_3 eluent
417 generator cartridge and a conductivity detector. Organic acids were analysed in the 0.2 µm
418 filtered sediment porewater using a Thermo RS3000 HPLC fitted with an Ultimate 3000 UV
419 detector. Separation was achieved over an Aminex HPX-87H organic acid column (Biorad, USA)
420 under isocratic conditions (0.05 mM H_2SO_4) at 60°C with a run time of 20 minutes. Organic
421 acids were compared to the retention time of known standards and the limit of detection for
422 acetate was determined to be 2.5 µM.

423 For the analysis of metabolites, sediment was spun down, the supernatant collected, diluted 1:1
424 in pure methanol, and filtered through 0.2 µm Teflon syringe filters. Extracts were separated
425 using Ultra High-Performance Liquid Chromatography (UHPLC) equipped with a hydrophilic
426 interaction liquid chromatography column (Syncronis HILIC, Thermo Fisher). A Thermo Fisher
427 Scientific Q-Exactive HF mass spectrometer in negative-mode electrospray ionization was used
428 to collect high-resolution full-scan MS data from 50-750 *m/z* at 240,000 resolution with an
429 automatic gain control (AGC) target of 3e6 and a maximum injection time of 200 ms. In addition,
430 benzoate ion (*m/z* 121.02943) was subjected to fragmentation using collision induced
431 dissociation (CID) with a collision energy of 10eV at 120,000 resolution (*m/z* 121.02943 >
432 77.03948). For CID experiments, an AGC target of 1e6 was used with a maximum injection time

433 of 100 ms. Metabolites were further identified using accurate mass and retention times of
434 standards using Thermo Xcalibur software and MAVEN freeware. Larger compound lists were
435 assigned identification using a combination of MAVEN and the KEGG database [60].

436 **DNA extraction and sequencing**

437 For the three sediment samples, DNA was extracted from 10 g of sediment using the PowerMax
438 Soil DNA Isolation Kit (12988-10, QIAGEN) according to the manufacturer's protocol with
439 minor modifications for the step of homogenization and cell lysis *i.e.*, cells were lysed in
440 PowerMax Bead Solution tubes for 45 s at 5.5 m s^{-1} using a Bead Ruptor 24 (OMNI
441 International). DNA concentrations were assessed using a Qubit 2.0 fluorometer (Thermo Fisher
442 Scientific, Canada). Metagenomic library preparation and DNA sequencing was conducted at the
443 Center for Health Genomics and Informatics in the Cumming School of Medicine, University of
444 Calgary. DNA fragment libraries were prepared by shearing genomic DNA using a Covaris
445 sonicator and the NEBNext Ultra II DNA library preparation kit (New England BioLabs). DNA
446 was sequenced on a ~40 Gb (*i.e.* 130 M reads) mid-output NextSeq 500 System (Illumina Inc.)
447 300 cycle (2 × 150 bp) sequencing run.

448 To provide a high-resolution microbial community profile, the three samples were also subjected
449 to 16S rRNA gene amplicon sequencing on a MiSeq benchtop sequencer (Illumina Inc.). DNA
450 was extracted from separate aliquots of the same sediment samples using the DNeasy
451 PowerLyzer PowerSoil kit (MO BIO Laboratories, a Qiagen Company, Carlsbad, CA, USA) and
452 used as the template for different PCR reactions. The v3-4 region of the bacterial 16S rRNA
453 gene and the v4-8 region of the archaeal 16S rRNA gene were amplified using the primer pairs
454 SD-Bact-0341-bS17/SD-Bact-0785-aA21 and SD-Arch-0519-aS15/SD-Arch-0911-aA20,

455 respectively [61] as described previously [20] on a ~15 Gb 600-cyce (2 × 300 bp) sequencing run (for
456 results see Figure S1).

457 **Metagenomic assembly and binning**

458 Raw reads were quality-controlled by (1) clipping off primers and adapters and (2) filtering out
459 artifacts and low-quality reads as described previously [62]. Filtered reads were assembled using
460 metaSPAdes version 3.11.0 [63] and short contigs (<500 bp) were removed. Sequence coverage
461 was determined by mapping filtered reads onto assembled contigs using BBmap version 36
462 (https://sourceforge.net/projects/bbmap/). Binning of metagenome contigs was performed using
463 MetaBAT version 2.12.1 (--minContig 1500) [64]. Contaminated contigs in the produced bins were
464 further removed based on genomic properties (GC, tetranucleotide signatures, and coverage) and
465 taxonomic assignments using RefineM version 0.0.22 [65]. Resulting bins were further examined
466 for contamination and completeness using CheckM version 1.0.8 with the lineage-specific
467 workflow [24].

468 **Annotation**

469 For MAGs, genes were called by Prodigal (-p meta) [66]. Metabolic pathways were predicted
470 against the KEGG GENES database using the GhostKOALA tool [67] and against the Pfam,
471 TIGRfam and custom HMM databases (https://github.com/banfieldlab/metabolic-hmms) using
472 MetaErg (https://sourceforge.net/projects/metaerg/). The dbCAN web server was used for
473 carbohydrate-active gene identification (cutoffs: coverage fraction: 0.40; e-value: 1e-18) [68].
474 Genes encoding proteases and peptidases were identified using BLASTp against the MEROPS
475 database release 12.0 (cutoffs: e-value, 1e-20; sequence identity, 30%) [69]. Genes involved in

anaerobic hydrocarbon degradation were identified using BLASTp against a custom database (Table S8) (cutoffs: e-value, 1e-20; sequence identity, 30%). Hydrogenases were identified and classified using a web-based search using the hydrogenase classifier HydDB [70].

Full-length 16S rRNA genes were reconstructed from metagenomic reads using phyloFlash version 3.1 (https://hrgv.github.io/phyloFlash/) together with the SILVA SSU 132 rRNA database [30]. Diversity calculations were based on separate 16S rRNA gene amplicon library results [20]. Functional and taxonomic McrA gpkgs were used to assess the diversity of methanogens against the metagenomic reads using GraftM with default parameters [71]. Genes encoding the catalytic subunits of hydrogenases, *dsrA*, *acsB*, *assA*, *nmsA* and *bssA* were retrieved from metagenomic reads through diamond BLASTx [72] queries against comprehensive custom databases [46, 70, 73] (cutoffs: e-value, 1e-10; sequence identity, 70%).

Phylogenetic analyses

For taxonomic classification of each MAG, two methods were used to produce genome trees that were then used to validate each other. In the first method the tree was constructed using concatenated proteins of up to 16 syntenic ribosomal protein genes following procedures reported elsewhere [74]; the second tree was constructed using concatenated amino acid sequences of up to 43 conserved single-copy genes following procedures described previously [75]. Both trees were calculated using FastTree version 2.1.9 (-lg -gamma) [76] and resulting phylogenies were congruent. Reference genomes for relatives were accessed from NCBI GenBank, including genomes selected from several recent studies representing the majority of candidate bacterial and archaeal phylogenetic groups [4, 65, 77-80]. The tree in Figure 2 was inferred based on concatenation of 43 conserved single-copy genes (Database S1). Specifically, it was built using RAxML

version 8 [81] implemented by the CIPRES Science Gateway [82] and it was called as follows: raxmlHPC-HYBRID -f a -n result -s input -c 25 -N 100 -p 12345 -m PROTCATLG -x 12345. The phylogeny resulting from RAxML is consistent with the taxonomic classification of MAGs that resulted from FastTree. Interactive tree of life (iTOL) version 3 [83] was used for tree visualization and modification.

For phylogenetic placements of functional genes, sequences were aligned using the MUSCLE algorithm [84] included in MEGA7 [85]. All positions with less than 95% site coverage were eliminated. Maximum likelihood phylogenetic trees were constructed in MEGA7 using a general time reversible substitution model and uniform rates among sites. These trees were bootstrapped with 100 replicates.

Taxonomic classification of MAGs inferred to belong to candidate phylum TA06 after phylogenetic analyses were additionally confirmed by performing classify workflow using GTDB-Tk version 0.0.6+ (https://github.com/Ecogenomics/GtdbTk).

Thermodynamic calculations

The values of Gibbs free energy of formation for substances were taken from Madigan et al. [86] and Dolfing et al. [55]. The pH used in all calculations was 8.0 as reported in a previous thermodynamic study of deep marine sediments [47], partial pressure was 300 atm based on water depths at the three sites (http://docs.bluerobotics.com/calc/pressure-depth/), and temperature was set as 4°C to represent deep sea conditions [87]. Calculations followed accepted protocols for determining reaction kinetics and thermodynamics [88].

Acknowledgements

The work was supported by a Genome Canada Genomics Applied Partnership Program (GAPP) grant to CRJH. I.A.L is supported by an Alberta Innovates Translational Health Chair. Metabolomics data were acquired by R.A.G. at the Calgary Metabolomics Research Facility (CMRF), which is supported by the International Microbiome Centre and the Canada Foundation for Innovation (CFI-JELF 34986). We thank Xiaoli Dong and Marc Strous for establishing bioinformatics workflow and pipelines, the Centre for Health Genomics and Informatics at University of Calgary for NextSeq sequencing, Alexander Probst for providing the database of 16 syntenic ribosomal proteins, and Nina Dombrowski and Brett Baker for providing a custom blast database for hydrocarbon degradation genes.

Data availability

DNA sequences (amplicon sequences, genomes and raw sequence reads) have been deposited in the NCBI BioProject database with accession number PRJNA415828 and PRJNASUB3936075 (https://www.ncbi.nlm.nih.gov/bioproject/). The authors declare that all other data supporting the findings of this study are available within the article and its supplementary information files, or from the corresponding authors upon request.

References

1. Petro, C., Starnawski, P., Schramm, A. & Kjeldsen, K.U. Microbial community assembly in marine sediments. *Aquat Microb Ecol* **79**, 177-195 (2017).
2. Vigneron, A. et al. Comparative metagenomics of hydrocarbon and methane seeps of the Gulf of Mexico. *Sci Rep* **7**, 16015 (2017).
3. Marshall, I.P.G., Karst, S.M., Nielsen, P.H. & Jørgensen, B.B. Metagenomes from deep Baltic Sea sediments reveal how past and present environmental conditions determine microbial community composition. *Mar Genomics* **37**, 58-68 (2018).
4. Dombrowski, N., Seitz, K.W., Teske, A.P. & Baker, B.J. Genomic insights into potential interdependencies in microbial hydrocarbon and nutrient cycling in hydrothermal sediments. *Microbiome* **5**, 106 (2017).
5. Lloyd, K.G. et al. Predominant archaea in marine sediments degrade detrital proteins. *Nature* **496**, 215-218 (2013).
6. Orsi, W.D. Ecology and evolution of seafloor and subseafloor microbial communities. *Nat Rev Microbiol* (2018).
7. Wang, Y. et al. Draft genome of an *Aerophobetes* bacterium reveals a facultative lifestyle in deep-sea anaerobic sediments. *Sci Bull* **61**, 1176-1186 (2016).
8. Orcutt, B.N., Sylvan, J.B., Knab, N.J. & Edwards, K.J. Microbial ecology of the dark ocean above, at, and below the seafloor. *Microbiol Mol Biol Rev* **75**, 361-422 (2011).
9. Inagaki, F. et al. Exploring deep microbial life in coal-bearing sediment down to ~2.5 km below the ocean floor. *Science* **349**, 420-424 (2015).
10. Jørgensen, B.B. & Marshall, I.P. Slow microbial life in the seabed. *Ann Rev Mar Sci* **8**, 311-332 (2016).
11. Jørgensen, B.B. & Boetius, A. Feast and famine--microbial life in the deep-sea bed. *Nat Rev Microbiol* **5**, 770-781 (2007).
12. Arndt, S. et al. Quantifying the degradation of organic matter in marine sediments: A review and synthesis. *Earth-Sci Rev* **123**, 53-86 (2013).
13. Orsi, W.D., Richards, T.A. & Francis, W.R. Predicted microbial secretomes and their target substrates in marine sediment. *Nat Microbiol* **3**, 32-37 (2018).

14. Brooks, J.M. et al. Deep-sea hydrocarbon seep communities: evidence for energy and nutritional carbon sources. *Science* **238**, 1138-1142 (1987).
15. Ijiri, A. et al. Deep-biosphere methane production stimulated by geofluids in the Nankai accretionary complex. *Sci Adv* **4**, eaao4631 (2018).
16. Ruff, S.E. et al. Global dispersion and local diversification of the methane seep microbiome. *Proc Natl Acad Sci U S A* **112**, 4015-4020 (2015).
17. Dong, X. et al. Fermentative Spirochaetes mediate necromass recycling in anoxic hydrocarbon-contaminated habitats. *ISME J* **12**, 2039-2050 (2018).
18. Lin, Y.-S. et al. Towards constraining H_2 concentration in subseafloor sediment: A proposal for combined analysis by two distinct approaches. *Geochim Cosmochim Acta* **77**, 186-201 (2012).
19. Sauvage, J., Flinders, A., Spivack, A. & D'Hondt, S. Global distribution of radiolytic H_2 production in marine sediment and implications for subsurface life. *AGU Fall Meeting Abstracts* (2017).
20. Chakraborty, A. et al. Thermophilic endospores associated with migrated thermogenic hydrocarbons in deep Gulf of Mexico marine sediments. *ISME J* **12**, 1895-1906 (2018).
21. Whiticar, M.J. Carbon and hydrogen isotope systematics of bacterial formation and oxidation of methane. *Chem Geol* **161**, 291-314 (1999).
22. Killops, S.D. & Aljuboori, M.A.H.A. Characterization of the Unresolved Complex Mixture (UCM) in the gas chromatograms of biodegraded petroleums. *Org Geochem* **15**, 147-160 (1990).
23. Gieg, L.M. & Toth, C.R.A. in Anaerobic Utilization of Hydrocarbons, Oils, and Lipids. (ed. M. Boll) 1-30 (Springer International Publishing, Cham; 2017).
24. Parks, D.H., Imelfort, M., Skennerton, C.T., Hugenholtz, P. & Tyson, G.W. CheckM: assessing the quality of microbial genomes recovered from isolates, single cells, and metagenomes. *Genome Res* **25**, 1043-1055 (2015).
25. Ley, R.E. et al. Unexpected diversity and complexity of the Guerrero Negro hypersaline microbial mat. *Appl Environ Microbiol* **72**, 3685-3695 (2006).
26. Baker, B.J., Lazar, C.S., Teske, A.P. & Dick, G.J. Genomic resolution of linkages in carbon, nitrogen, and sulfur cycling among widespread estuary sediment bacteria. *Microbiome* **3**, 14 (2015).

27. Hu, P. et al. Genome-resolved metagenomic analysis reveals roles for candidate phyla and other microbial community members in biogeochemical transformations in oil reservoirs. *MBio* **7**, e01669-01615 (2016).
28. Sieber, C.M.K. et al. Recovery of genomes from metagenomes via a dereplication, aggregation and scoring strategy. *Nat Microbiol* **3**, 836-843 (2018).
29. Parks, D.H. et al. A standardized bacterial taxonomy based on genome phylogeny substantially revises the tree of life. *Nat Biotechnol* (2018).
30. Quast, C. et al. The SILVA ribosomal RNA gene database project: improved data processing and web-based tools. *Nucleic Acids Res* **41**, D590-596 (2013).
31. Bradley, J.A., Amend, J.P. & LaRowe, D.E. Necromass as a limited source of energy for microorganisms in marine sediments. *J Geophys Res-Biogeo* **123**, 577-590 (2018).
32. Lipp, J.S., Morono, Y., Inagaki, F. & Hinrichs, K.U. Significant contribution of Archaea to extant biomass in marine subsurface sediments. *Nature* **454**, 991-994 (2008).
33. Boll, M. & Heider, J. in Handbook of Hydrocarbon and Lipid Microbiology. (ed. K.N. Timmis) 1011-1024 (Springer Berlin Heidelberg, Berlin, Heidelberg; 2010).
34. Tan, B. et al. Comparative analysis of metagenomes from three methanogenic hydrocarbon-degrading enrichment cultures with 41 environmental samples. *ISME J* **9**, 2028-2045 (2015).
35. Meckenstock, R.U. et al. Anaerobic degradation of benzene and polycyclic aromatic hydrocarbons. *J Mol Microbiol Biotechnol* **26**, 92-118 (2016).
36. Laso-Perez, R. et al. Thermophilic archaea activate butane via alkyl-coenzyme M formation. *Nature* **539**, 396-401 (2016).
37. Rabus, R. et al. Anaerobic Microbial Degradation of Hydrocarbons: From Enzymatic Reactions to the Environment. *J Mol Microbiol Biotechnol* **26**, 5-28 (2016).
38. Schouw, A. et al. *Abyssivirga alkaniphila* gen. nov., sp. nov., an alkane-degrading, anaerobic bacterium from a deep-sea hydrothermal vent system, and emended descriptions of *Natranaerovirga pectinivora* and *Natranaerovirga hydrolytica*. *Int J Syst Evol Microbiol* **66**, 1724-1734 (2016).
39. Khelifi, N. et al. Anaerobic oxidation of long-chain n-alkanes by the hyperthermophilic sulfate-reducing archaeon, *Archaeoglobus fulgidus*. *ISME J* **8**, 2153-2166 (2014).

624 40. Porter, A.W. & Young, L.Y. in Advances in Applied Microbiology, Vol. 88. (eds. S.
625 Sariaslani & G.M. Gadd) 167-203 (Academic Press, 2014).
626 41. Dong, X. et al. Reconstructing metabolic pathways of a member of the genus
627 *Pelotomaculum* suggesting its potential to oxidize benzene to carbon dioxide with direct
628 reduction of sulfate. *FEMS Microbiol Ecol* **93**, fiw254-fiw254 (2017).
629 42. Holmes, D.E., Risso, C., Smith, J.A. & Lovley, D.R. Genome-scale analysis of anaerobic
630 benzoate and phenol metabolism in the hyperthermophilic archaeon *Ferroglobus*
631 *placidus*. *ISME J* **6**, 146-157 (2012).
632 43. Beulig, F., Røy, H., Glombitza, C. & Jørgensen, B.B. Control on rate and pathway of
633 anaerobic organic carbon degradation in the seabed. *Proc Natl Acad Sci U S A* **115**, 367-
634 372 (2018).
635 44. Sewell, H.L., Kaster, A.K. & Spormann, A.M. Homoacetogenesis in Deep-Sea
636 *Chloroflexi*, as inferred by single-cell genomics, provides a link to reductive
637 dehalogenation in terrestrial *Dehalococcoidetes*. *MBio* **8** (2017).
638 45. He, Y. et al. Genomic and enzymatic evidence for acetogenesis among multiple lineages
639 of the archaeal phylum *Bathyarchaeota* widespread in marine sediments. *Nat Microbiol* **1**,
640 16035 (2016).
641 46. Adam, P.S., Borrel, G. & Gribaldo, S. Evolutionary history of carbon monoxide
642 dehydrogenase/acetyl-CoA synthase, one of the oldest enzymatic complexes. *Proc Natl*
643 *Acad Sci U S A* **115**, E1166-E1173 (2018).
644 47. Lever, M.A. Acetogenesis in the energy-starved deep biosphere - a paradox? *Front*
645 *Microbiol* **2**, 284 (2011).
646 48. Yu, T. et al. Growth of sedimentary *Bathyarchaeota* on lignin as an energy source. *Proc*
647 *Natl Acad Sci U S A* **115**, 6022-6027 (2018).
648 49. Berney, M., Greening, C., Conrad, R., Jacobs, W.R., Jr. & Cook, G.M. An obligately
649 aerobic soil bacterium activates fermentative hydrogen production to survive reductive
650 stress during hypoxia. *Proc Natl Acad Sci U S A* **111**, 11479-11484 (2014).
651 50. Ma, K., Hao, Z. & Adams, M.W.W. Hydrogen production from pyruvate by enzymes
652 purified from the hyperthermophilic archaeon, *Pyrococcus furiosus*: A key role for
653 NADPH. *FEMS Microbiol Lett* **122**, 245-250 (1994).

654 51. Greening, C. et al. Genomic and metagenomic surveys of hydrogenase distribution
655 indicate H_2 is a widely utilised energy source for microbial growth and survival. *ISME J*
656 **10**, 761 (2015).
657 52. Wagner, T., Koch, J., Ermler, U. & Shima, S. Methanogenic heterodisulfide reductase
658 (HdrABC-MvhAGD) uses two noncubane [4Fe-4S] clusters for reduction. *Science* **357**,
659 699-703 (2017).
660 53. Adhikari, R.R. et al. Hydrogen utilization potential in subsurface sediments. *Front*
661 *Microbiol* **7**, 8 (2016).
662 54. Kawai, M. et al. High frequency of phylogenetically diverse reductive dehalogenase-
663 homologous genes in deep subseafloor sedimentary metagenomes. *Front Microbiol* **5**, 80
664 (2014).
665 55. Dolfing, J., Larter, S.R. & Head, I.M. Thermodynamic constraints on methanogenic
666 crude oil biodegradation. *ISME J* **2**, 442-452 (2008).
667 56. Canfield, D.E., Thamdrup, B. & Hansen, J.W. The anaerobic degradation of organic
668 matter in Danish coastal sediments: iron reduction, manganese reduction, and sulfate
669 reduction. *Geochim Cosmochim Acta* **57**, 3867-3883 (1993).
670 57. Liu, Y.F. et al. Metabolic capability and in situ activity of microorganisms in an oil
671 reservoir. *Microbiome* **6**, 5 (2018).
672 58. Colman, D.R., Poudel, S., Stamps, B.W., Boyd, E.S. & Spear, J.R. The deep, hot
673 biosphere: Twenty-five years of retrospection. *Proc Natl Acad Sci U S A* **114**, 6895-6903
674 (2017).
675 59. Bernard, B.B. et al. Surface geochemical exploration and heat flow surveys in fifteen (15)
676 frontier Indonesian basins. *Thirty-Second Annual Convention & Exhibition May 2008*
677 (2008).
678 60. Kanehisa, M., Sato, Y., Kawashima, M., Furumichi, M. & Tanabe, M. KEGG as a
679 reference resource for gene and protein annotation. *Nucleic Acids Res* **44**, D457-462
680 (2016).
681 61. Klindworth, A. et al. Evaluation of general 16S ribosomal RNA gene PCR primers for
682 classical and next-generation sequencing-based diversity studies. *Nucleic Acids Research*
683 **41**, e1-e1 (2013).

62. Kleiner, M. et al. Assessing species biomass contributions in microbial communities via metaproteomics. *Nat Commun* **8**, 1558 (2017).
63. Nurk, S., Meleshko, D., Korobeynikov, A. & Pevzner, P.A. metaSPAdes: a new versatile metagenomic assembler. *Genome Res* **27**, 824-834 (2017).
64. Kang, D.D., Froula, J., Egan, R. & Wang, Z. MetaBAT, an efficient tool for accurately reconstructing single genomes from complex microbial communities. *PeerJ* **3**, e1165 (2015).
65. Parks, D.H. et al. Recovery of nearly 8,000 metagenome-assembled genomes substantially expands the tree of life. *Nat Microbiol* **2**, 1533-1542 (2017).
66. Hyatt, D. et al. Prodigal: prokaryotic gene recognition and translation initiation site identification. *BMC Bioinformatics* **11**, 119 (2010).
67. Lombard, V., Golaconda Ramulu, H., Drula, E., Coutinho, P.M. & Henrissat, B. The carbohydrate-active enzymes database (CAZy) in 2013. *Nucleic Acids Res* **42**, D490-495 (2014).
68. Yin, Y. et al. dbCAN: a web resource for automated carbohydrate-active enzyme annotation. *Nucleic Acids Res* **40**, W445-451 (2012).
69. Rawlings, N.D. et al. The MEROPS database of proteolytic enzymes, their substrates and inhibitors in 2017 and a comparison with peptidases in the PANTHER database. *Nucleic Acids Res* **46**, D624-D632 (2018).
70. Søndergaard, D., Pedersen, C.N. & Greening, C. HydDB: A web tool for hydrogenase classification and analysis. *Sci Rep* **6**, 34212 (2016).
71. Boyd, J.A., Woodcroft, B.J. & Tyson, G.W. GraftM: a tool for scalable, phylogenetically informed classification of genes within metagenomes. *Nucleic Acids Res* **46**, e59 (2018).
72. Buchfink, B., Xie, C. & Huson, D.H. Fast and sensitive protein alignment using DIAMOND. *Nat Methods* **12**, 59 (2014).
73. Anantharaman, K. et al. Expanded diversity of microbial groups that shape the dissimilatory sulfur cycle. *ISME J* **12**, 1715-1728 (2018).
74. Tully, B.J., Sachdeva, R., Graham, E.D. & Heidelberg, J.F. 290 metagenome-assembled genomes from the Mediterranean Sea: a resource for marine microbiology. *PeerJ* **5**, e3558 (2017).

75. Kato, S. et al. Genome-enabled metabolic reconstruction of dominant chemosynthetic colonizers in deep-sea massive sulfide deposits. *Environ Microbiol* **20**, 862-877 (2018).
76. Price, M.N., Dehal, P.S. & Arkin, A.P. FastTree 2--approximately maximum-likelihood trees for large alignments. *PLoS One* **5**, e9490 (2010).
77. Anantharaman, K. et al. Thousands of microbial genomes shed light on interconnected biogeochemical processes in an aquifer system. *Nat Commun* **7**, 13219 (2016).
78. Zaremba-Niedzwiedzka, K. et al. Asgard archaea illuminate the origin of eukaryotic cellular complexity. *Nature* **541**, 353-358 (2017).
79. Probst, A.J. et al. Differential depth distribution of microbial function and putative symbionts through sediment-hosted aquifers in the deep terrestrial subsurface. *Nat Microbiol* **3**, 328-336 (2018).
80. Hug, L.A. et al. A new view of the tree of life. *Nat Microbiol* **1**, 16048 (2016).
81. Stamatakis, A. RAxML version 8: a tool for phylogenetic analysis and post-analysis of large phylogenies. *Bioinformatics* **30**, 1312-1313 (2014).
82. Miller, M.A., Pfeiffer, W. & Schwartz, T. Creating the CIPRES Science Gateway for inference of large phylogenetic trees. *2010 Gateway Computing Environments Workshop (GCE)*, 1-8 (2010).
83. Letunic, I. & Bork, P. Interactive tree of life (iTOL) v3: an online tool for the display and annotation of phylogenetic and other trees. *Nucleic Acids Res* **44**, W242-245 (2016).
84. Edgar, R.C. MUSCLE: multiple sequence alignment with high accuracy and high throughput. *Nucleic Acids Res* **32**, 1792-1797 (2004).
85. Kumar, S., Stecher, G. & Tamura, K. MEGA7: Molecular Evolutionary Genetics Analysis Version 7.0 for Bigger Datasets. *Mol Biol Evol* **33**, 1870-1874 (2016).
86. Madigan, M.T., Martinko, J.M. & Parker, J. Brock biology of microorganisms, Vol. 13. (Pearson, 2017).
87. Xu, W.Y., Lowell, R.P. & Peltzer, E.T. Effect of seafloor temperature and pressure variations on methane flux from a gas hydrate layer: Comparison between current and late Paleocene climate conditions. *J Geophys Res-Sol Ea* **106**, 26413-26423 (2001).
88. Dolfing, J. in Hydrocarbon and Lipid Microbiology Protocols. (eds. T.J. McGenity, K.N. Timmis & B. Nogales Fernández) 155-163 (Springer Berlin Heidelberg, Berlin, Heidelberg; 2015).

Tables and Figures

Table 1 Geochemical description of sediment samples from Sites E26, E29 and E44. TSF Max: total scanning fluorescence maximum intensity. UCM: uncharacterized complex mixture. Σn-Alk: sum of C_{15}-C_{34} n-alkanes. ΣAlk Gas: total alkane gases. C_{2+} Alk: sum of alkane gases larger than methane. T/D: thermogenic/diagenetic n-alkane ratio. BDL: below detection limit. NA: not analyzed.

Core ID	*Site E26*	*Site E29*	*Site E44*
Latitude (N)	26.59	27.43	26.28
Longitude (W)	87.51	86.01	86.81
Water depth (km)	2.8	3.2	3.0
Sulfate (mM)	20.01	33.73	31.72
Benzoate (nM)	93.6	22.6	161.7
Succinate (nM)	11.7	5.0	16.6
Acetate (μM)	BDL	BDL	BDL
Chloride (g L^{-1})	21.04	20.15	21.05
Total Scanning Fluorescence MAX	57326.7	26738.3	13502.3
Unresolved Complex Mixture (μg g^{-1})	32	13	7.3
Σn-Alkanes (ng g^{-1})	2845.3	2527	1045
Thermogenic/Diagenetic Ratio	1.0	2.6	0.8
ΣAlkane Gas (ppm)	9	36012	9.9
C_{2+} Alkanes (ppm)	0.3	17.5	0.5
$C_1/(C_2+C_3)$	NA	3974.2	NA
$\delta^{13}CH_4$ (‰, vs. PDB)	NA	-85.1	NA
H_2 (ppm)	BDL	BDL	BDL

751 **Figure 1 Relative frequency of metagenomic sequence reads for different marker genes at**
752 **Sites E26, E29 and E44.** (a) Community composition based on reconstruction of full-length 16S
753 rRNA genes from the metagenomes. Eukaryotes and unassigned reads are not shown. (b)
754 Relative occurrences of hydrogenases with different metal cofactors. (c) Relative occurrences of
755 different subtypes of NiFe hydrogenases. (d) Relative occurrences of *mcrA* genes indicative of
756 different types of methanogenesis.

757 **Figure 2 Phylogenetic placement of 82 reconstructed metagenome-assembled genomes.** A
758 maximum-likelihood phylogenomic tree was built based on concatenated amino acid sequences
759 of 43 conserved single copy genes using RAxML with the PROTGAMMALG model. Sequences
760 of *Altiarchaeales* ex4484_43 were used as an outgroup. The scale bar represents 1 amino acid
761 substitution per sequence position. Bootstrap values > 70% are indicated. Blue for Site E26
762 (E26_binX), red for Site E29 (E29_binY), and green for Site E44 (E44_binZ).

763 **Figure 3 Identification of functional genes or pathways present in MAGs.** The presence of
764 genes or pathways are indicated by orange shaded boxes. Gene names: Aor, aldehyde:ferredoxin
765 oxidoreductase; Kor, 2-oxoglutarate/2-oxoacid ferredoxin oxidoreductase; Por,
766 pyruvate:ferredoxin oxidoreductase; Ior, indolepyruvate ferredoxin oxidoreductase; GHs,
767 glycoside hydrolases; AssA, catalytic subunit of alkylsuccinate synthase. CmdA, catalytic
768 subunit of p-cymene dehydrogenase; AhyA, catalytic subunit of alkane C2-methylene
769 hydroxylase; H_2ase, hydrogenase; DsrAB, dissimilatory sulfite reductase. Pathways were
770 indicated as being present if at least five genes in the Embden-Meyerhof-Parnas pathway, three
771 genes in the beta-oxidation pathway, four genes in the Wood-Ljungdahl pathway, and six genes
772 in the TCA cycle were detected. Additional details for the central benzoyl-CoA degradation

773 pathway can be found in Figure 4. Lactate and ethanol fermentation are indicated if genes
774 encoding respective dehydrogenases were detected. More details about these functional genes
775 and pathways can be found in the text and in Table S6.

776 **Figure 4 Evidence for anaerobic hydrocarbon degradation in MAGs.** (a) Phylogenetic
777 relationship of identified genes in MAGs with currently known alkyl-arylalkylsuccinate
778 synthases based on the respective catalytic alpha-subunits. Gene names: Ass/Mas, n-alkanes (1-
779 methylalkyl) succinate synthase; Nms, 2-naphthylmethyl succinate synthase; Bss, benzyl
780 succinate synthase; Ibs, 4-isopropylbenzyl succinate synthase; Hbs, 4-hydroxybenzyl succinate
781 synthase. Sequences of pyruvate formate lyase (Pfl) from *E. coli* were used as an outgroup. The
782 scale bar represents 0.1 amino acid substitutions per sequence position. Bootstrap values > 70%
783 are indicated. The full sequences can be found in Text S1. (b) Summary of identified enzymes
784 involved in central benzoyl-CoA processing in anaerobic aromatic hydrocarbon biodegradation.
785 The MAGs were shown only if it was at least partially complete (presence of at least three
786 subunits within one cluster for BcrABCD). Presence of genes or pathways are indicated by green
787 boxes. Gene names: Bcr, benzoyl-CoA reductase; Oah, 6-oxo-cyclohex-1-ene-carbonyl-CoA
788 hydrolase; Dch, cyclohex-1,5-diencarbonyl-CoA hydratase; Had, 6-hydroxycyclohex-1-ene-1-
789 carbonyl-CoA dehydrogenases.

790 **Figure 5 Thermodynamic constraints on anaerobic benzoate and hexadecane degradation**
791 **in deep sea sediments.** Two possible scenarios are illustrated depending on the end products
792 based on metabolic predictions in Figure 3: (1) fermentation with production of hydrogen and
793 acetate, and (2) fermentation with production of acetate alone. Thermodynamics for each
794 reaction are indicated by a line in its corresponding color. If $\Delta G' < 0$, the reaction is energetically

795 favorable (yellow-shaded area), and if $\Delta G' > 0$ the reaction is assumed not to occur. The graph
796 shows that $\Delta G'$ for hexadecane fermentation to acetate alone (green reaction) will not reach
797 negative values unless the concentration for acetate is extremely low (far lower than the
798 detection limit for acetate of 2.5 μM in this study, see dash line) such that the other three
799 reactions are more realistic scenarios for anaerobic hydrocarbon degradation in the marine
800 sediments studied here.

801 **Figure 6 Common potential organotrophic and hydrogenotrophic pathways in three**
802 **hydrocarbon-impacted microbial communities as inferred from metagenomics and**
803 **metabolomics.**

804 **Figure 1**

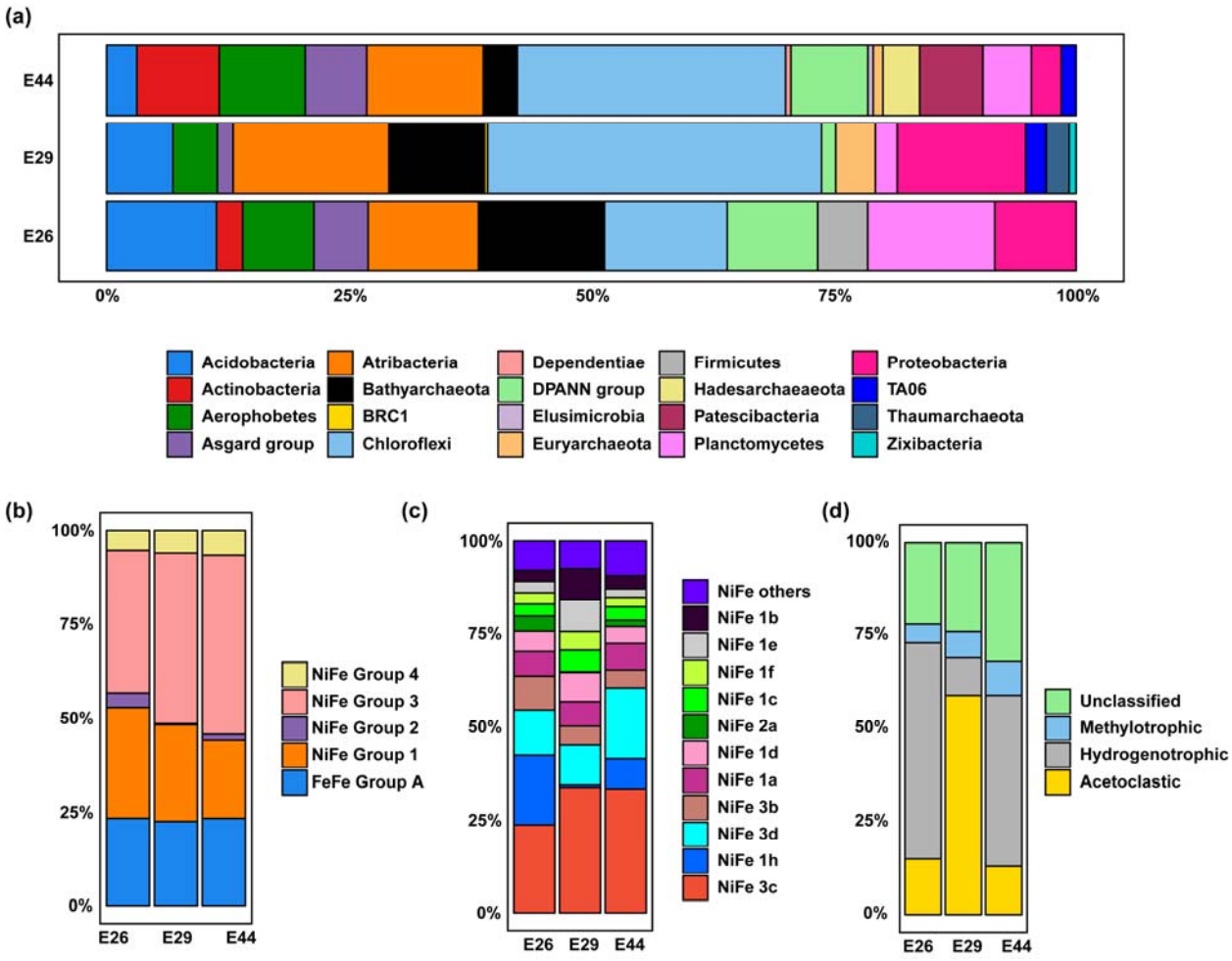

805

806 **Figure 2**

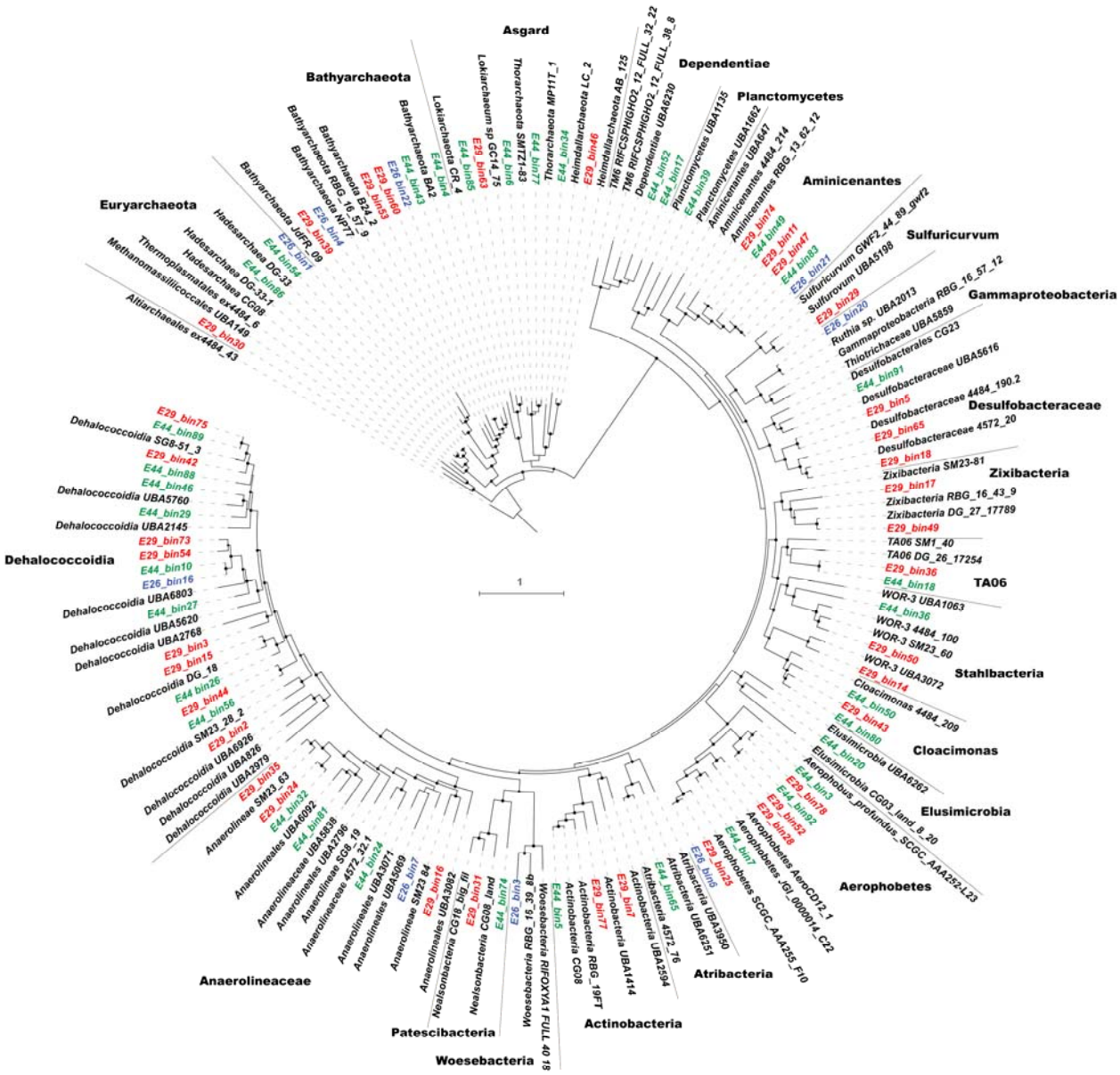

807

808 **Figure 3**

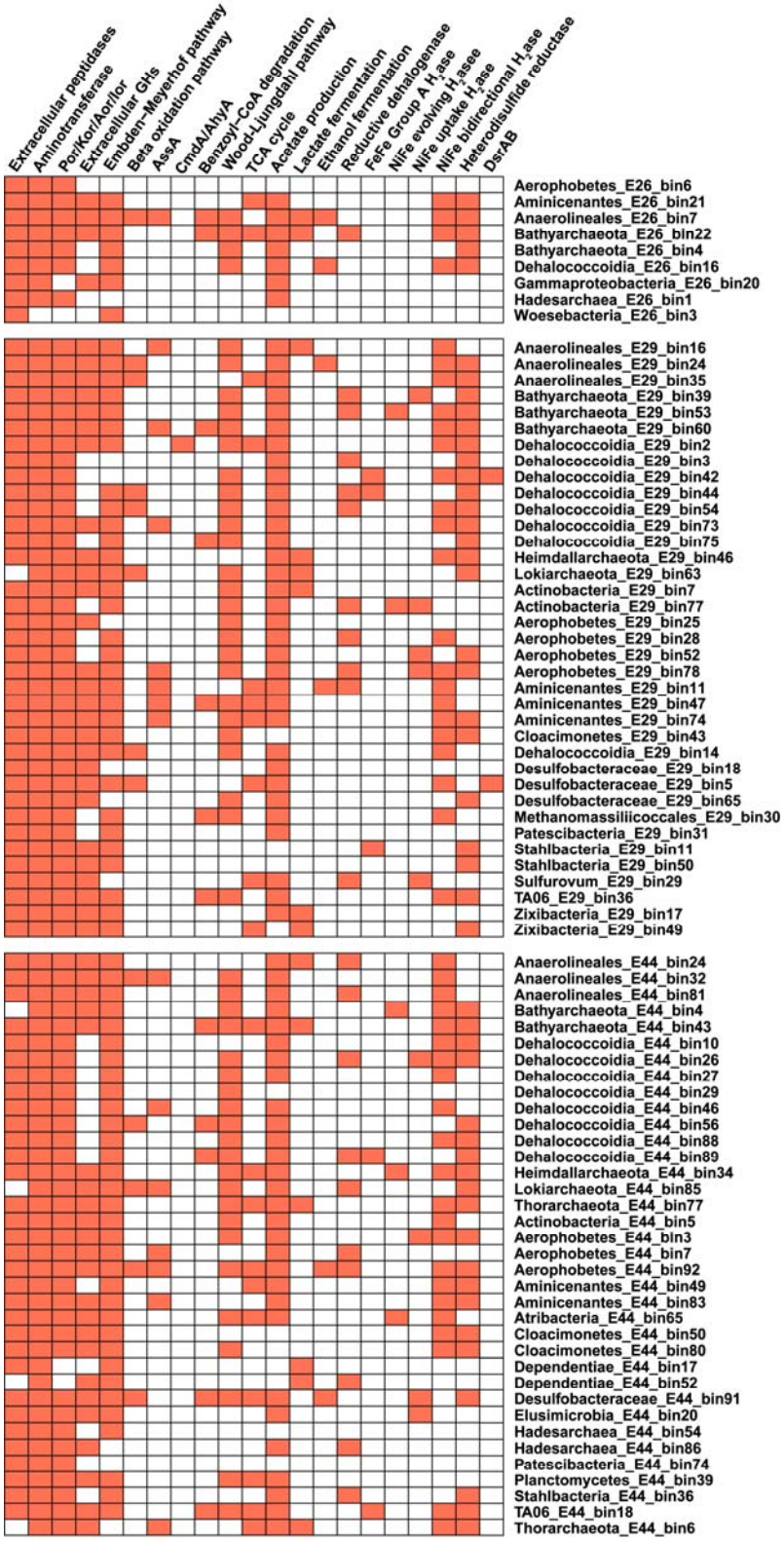

809

Figure 4

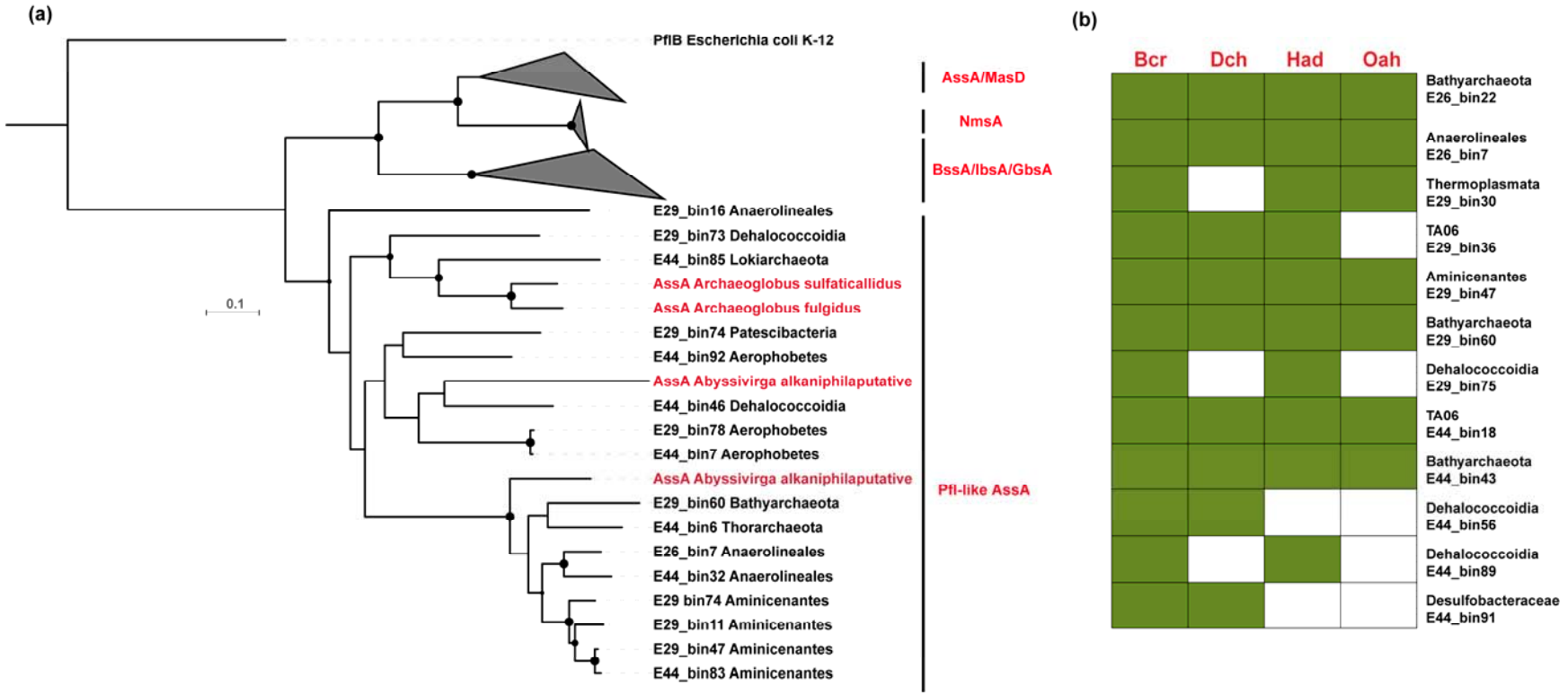

812 **Figure 5**

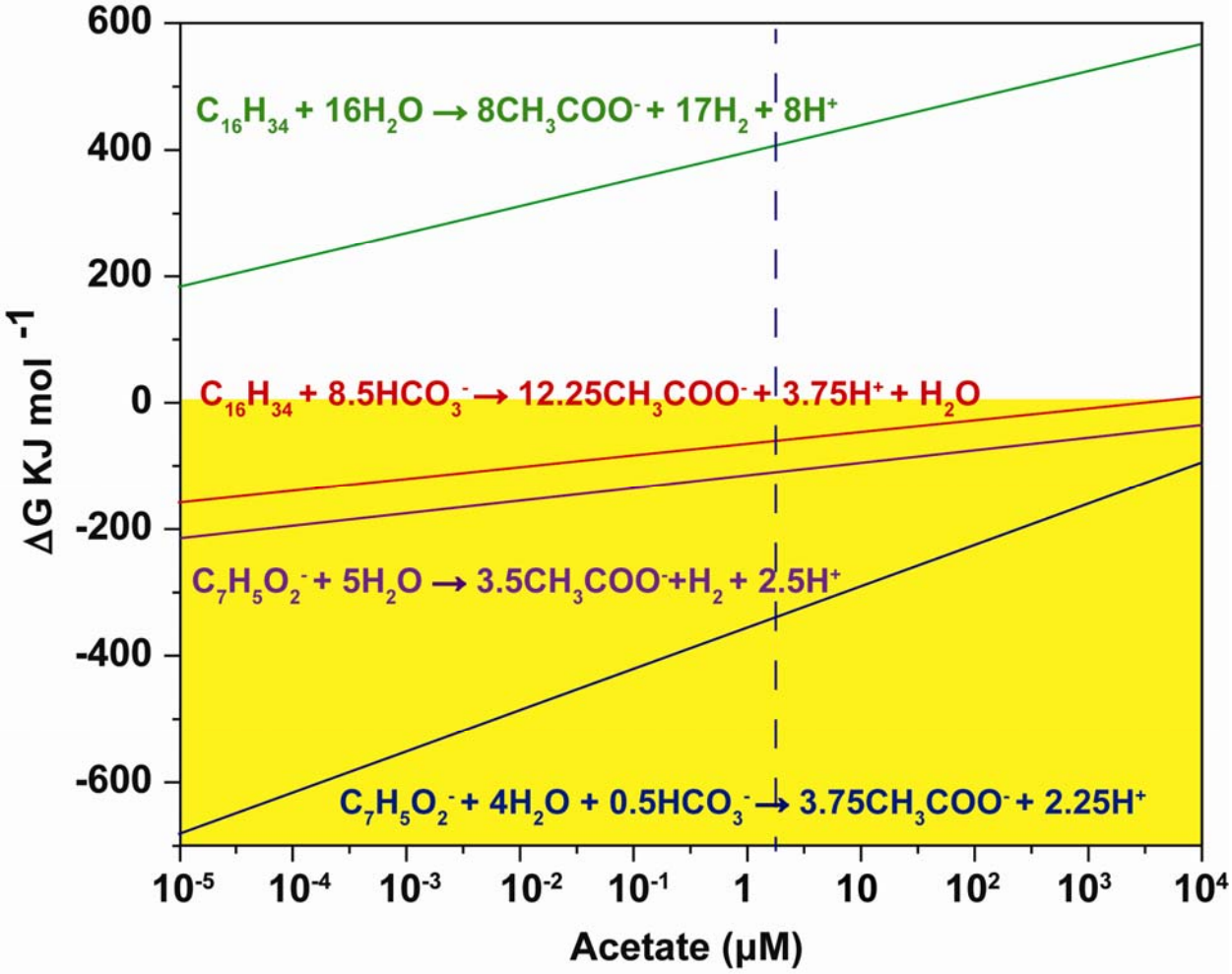

813

814 **Figure 6**

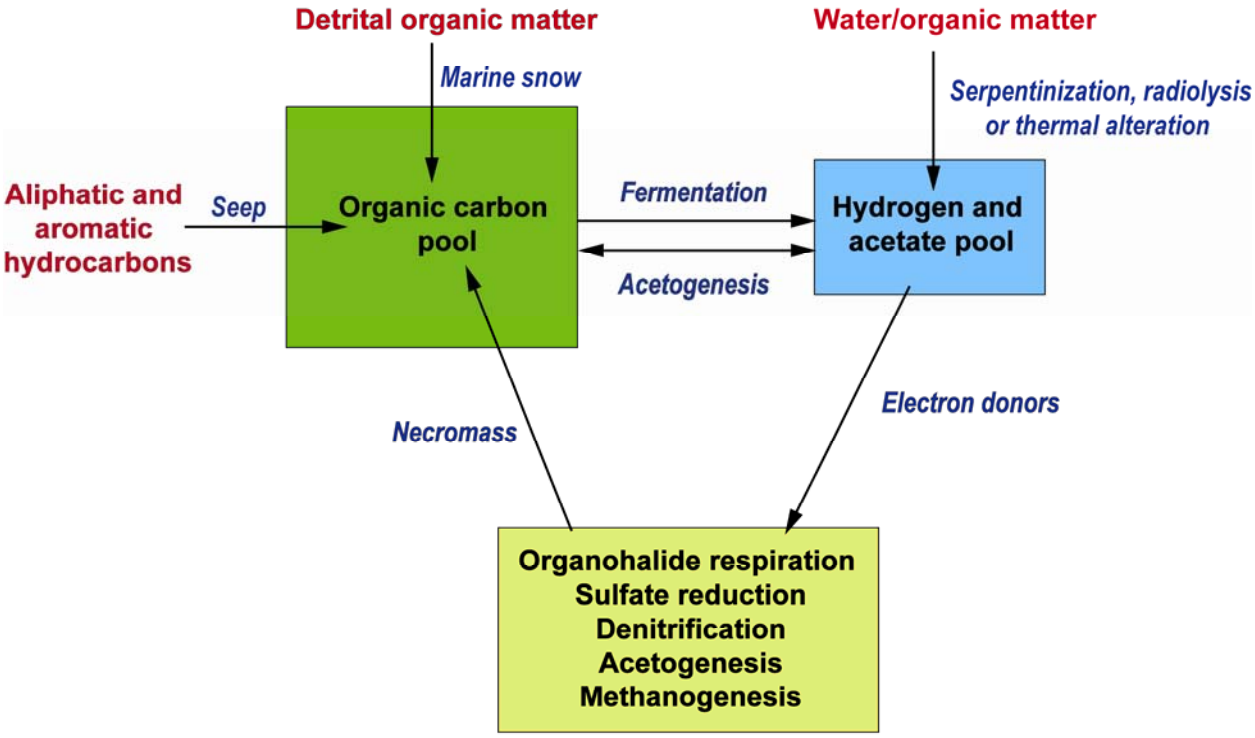

815

816